The Search for Endogenous Lenalidomide in Cell Lines

The search for endogenous lenalidomide in cell lines

by

Emma Catherine Fink

Submitted in Partial Fulfillment of the Requirements for the M.D. Degree with Honors in a Special Field at Harvard Medical School

Feb 10, 2020

Abstract

Thalidomide and its derivatives lenalidomide and pomalidomide bind to cereblon (CRBN), the substrate adaptor of the $CRL4^{CRBN}$ E3 ubiquitin ligase and induce the recruitment and ubiquitination of specific target proteins, ultimately resulting in their degradation by the proteasome. Recent crystal structures demonstrate that thalidomide derivatives recruit substrates by acting as a "molecular glue," bridging the protein interfaces of CRBN and recruited substrates including the transcription factors Ikaros (IKZF1) and Aiolos (IKZF3). This mechanism is analogous to that of multiple classes of plant hormones, but endogenous compounds that bind to E3 ligases to recruit substrates have not been described in mammalian cells. We hypothesized that there might exist a similar system in mammalian cellls wherein an endogenous small molecule would bind to CRBN to induce the recruitment and ubiquitination of IKZF1 and IKZF3. We sought a cellular context with proteasomal degradation of IKZF3 that was blunted by treatment with glutarimide, a small molecule competitive inhibitor of the CRBN thalidomide-binding pocket. We found that the T-cell acute lymphoblastic leukemia cell line Molt-4 met these criteria. Metabolites extracted from Molt-4 cells induced CRBN-dependent degradation of IKZF3 in reporter cell lines, suggesting activity due to a small molecule rather than a post-translational modification. Several biochemical assays confirmed direct interaction between the extracted metabolites and CRBN. Extracted metabolites induced the recruitment and ubiquitination of IKZF1 *in vitro* and also induced the degradation of additional recently described IMiD substrates RNF166 and ZNF692. Extraction and purification methods were developed to isolate this activity, dubbed eLen. Finally, an unbiased screen of a cell line library was undertaken to identify additional cellular contexts in which this activity could be identified. We identified eLen production in the renal medullary carcinoma cell line Peds005TSusp, which could be altered by changes in the expression of the tumor suppressor SMARCB1.

Table of Contents:

Glossary

ACN – acetonitrile

eLen – endogenous lenalidomide (term for endogenous IKZF3-degrading activity)

CRBN – cereblon

CK1α – casein kinase 1a

HPLC-MS – high performance liquid chromatography- mass spectrometry

IKZF1 – Ikaros

IKZF3 – Aiolos

Len – lenalidomide

Pom – pomalidomide

T-ALL – T cell acute lymphoblastic leukemia

TBS – tris buffered saline

TR-FRET – time resolved fluorescence resonance energy transfer

Contributions

The IKZF1 ubiquitination assay was performed by Hojong Yoon (Eric Fischer group). TR-FRET assays were performed with Gerog Petzold (Nico Thoma group). HPLC-MS was performed with the help of Emily Mevers (John Clardy group), Julian Pacheco (Clary Clish group), and Steve Carr's group. Dylan Adams provided technical assistance throughout. Mikolaj Slabicki provided assistance with metabolite optimization, preparation, and CRISPR constructs. Andy Hong (Bill Hahn group) provided the Peds005TSusp cell line, derivatives, and SMARCB1 construct. The introduction is based in part on a review by Emma Fink and Ben Ebert (1).

Introduction

Thalidomide, once infamous for its teratogenic effects, and its derivatives lenalidomide and pomalidomide (Figure 1a) have found new clinical utility as highly effective treatments for multiple myeloma (2-6), other B cell neoplasms (7-9), and myelodysplastic syndrome (MDS) with del(5q) (10-12). These molecules, together known as immunomodulatory drugs (IMiDs), bind to cereblon (CRBN), the substrate adaptor of the $CRL4^{CRBN}$ E3 ubiquitin ligase, and induce the recruitment and ubiquitination of specific target proteins, ultimately resulting in their degradation by the proteasome (13-15).

The modulation of an E3 ubiquitin ligase to specifically target substrate proteins for degradation is a novel drug mechanism. However, several plant hormones, including auxin (16) and jasmonate (17), act similarly on E3 ligases to induce targeted degradation of transcription factors. Structural evidence suggests that, like these plant hormones, lenalidomide acts as a "molecular glue" to bridge the E3-substrate interface (18, 19). Although such regulation of E3 ligases by endogenous small molecule hormones has not been reported in mammalian cells, several features of lenalidomide suggest that it could be imitating an endogenous regulator. The first is that IKZF1 and IKZF3 interact with CRBN, albeit more weakly, in the absence of lenalidomide, suggesting that they may be endogenous targets of the ligase (13). The second is lenalidomide's substrate specificity, as it induces degradation of only a small number of endogenous proteins and primarily targets transcription factors, similar to plant hormones (20). Given the highly conserved nature of the ubiquitin-proteasome system, it seems likely that lenalidomide may imitate an endogenous regulatory mechanism controlling the activity of $CRL4^{CRBN}$. If this is the case, it could provide the first example of an addition layer of regulation through metabolite-E3 ligase interactions in human cells, providing significant opportunities to

further our understanding of protein degradation and harness these endogenous mechanisms in future drug development. This thesis attempts to characterize whether such an endogenous compound might exist in cell lines.

Lenalidomide modulates the CRL4^{CRBN} E3 ubiquitin ligase

In 2010, Ito et al. (21) identified CRBN as the primary molecular target of thalidomide. CRBN is the substrate adaptor of the CRL4^{CRBN} E3 ubiquitin ligase, a cullin-ring ligase composed of damaged DNA binding protein 1 (DDB1), cullin 4a (CUL4A), and regulator of cullins 1 (ROC1) (Figure 1b).

Proteome-wide surveys revealed that the transcription factors IKZF1 and IKZF3 are selectively ubiquitinated and degraded in the presence of lenalidomide (13, 15). These transcription factors are essential in the B-cell lineage, so their degradation explains the clinical efficacy of thalidomide derivatives in multiple myeloma. Additional proteomic studies identified casein kinase 1A1 (gene: *CSNK1A1* protein: CK1α) as a lenalidomide target in myeloid cells and CK1α is ubiquitinated and degraded in a CRBN-dependent manner (22). *CSNK1A1* is encoded within the del(5q) common deleted region and is expressed at haploinsufficient levels in del(5q) cells (23, 24). Lenalidomide-induced degradation of CK1α triggers the death of haploinsufficient del(5q) cells but not wild-type cells, providing a mechanistic explanation for lenalidomide's efficacy in this condition (22).

Biochemical investigations revealed that IMiDs induce the recruitment of IKZF1, IKZF3, and CK1α to CRL4^{CRBN} and promote their ubiquitination by this complex (13, 15, 22). Once ubiquitinated, IKZF1, IKZF3, and CK1α are degraded by the proteasome, leading to decreased protein levels. Lenalidomide-induced ubiquitination of these substrates can be recapitulated *in vitro*, confirming direct interaction between these targets and CRBN. Lenalidomide-induced

substrate recognition is exquisitely specific, as other highly homologous members of the Ikaros and casein kinase families are not affected. A 60 amino acid region within the IKZF3 protein constitutes a lenalidomide-inducible degron and this region is nearly identical between IKZF1 and IKZF3. Fusion of this sequence to a heterologous protein is sufficient for lenalidomide-induced degradation but single point mutations in this region, including Q147H, can abrogate the lenalidomide response (13). Based on this finding, we created flow-cytometry based reporters of post-translational protein stability in which the fluorescence of enhanced green fluorescent protein (eGFP) tagged with a region of protein of interest is compared to an untagged mCherry. These reporters (known as Artichoke derivatives) are used extensively throughout this thesis, both as measures of endogenous proteasomal degradation and protein degradation triggered in 293T reporter cells by drug or metabolite treatment.

Recently published crystal structures of the tertiary CRBN-DDB1-lenalidomide-substrate complex provide further mechanistic insight into how IMiDs act on $CRL4^{CRBN}$ (18, 25-27). IMiDs bind CRBN through their shared glutarimide ring, leaving portions of their variable pthaloyl ring solvent-exposed (18, 19). Substrates are recruited to the CRBN-IMiD interface in the presence of drug and make contacts with both the surface of CRBN and the IMiD. Extensive protein-protein interactions between CRBN and substrate are required and IMiDs have little affinity for recruited substrates in the absence of CRBN. A β-hairpin contained between adjacent zinc fingers in IKZF1 and IKZF3 is critical for recognition and a β-loop in casein kinase shares a similar secondary structure (26). Additional zinc finger proteins which share this β-hairpin, such as ZFP91 and ZNF692, have recently been observed to undergo IMID-induced degradation and many of these proteins are putative transcription factors (25, 28). Thus, IMiDs act as a novel "molecular glue," bridging the interface between CRBN and recruited substrates.

Structural alterations in the solvent exposed ring of IMiD derivatives can alter their substrate specificity (22, 25). In pomalidomide, an additional carbonyl group creates steric hindrance with the CRBN binding pocket upon CK1α recruitment, explaining the lower affinity for this substrate (26). Similarly, a novel thalidomide analogue, CC-122 has a strong effect on IKZF1 and IKZF3 without any significant effect on CK1α protein levels (22). More significant structural alterations can induce the recruitment of novel substrates, as in the case of the thalidomide derivative CC-885 and the translation termination factor GSPT1 (29). Thus, changes in the chemical structure of thalidomide derivatives can change the repertoire of recruited substrates. Importantly, all known CRBN-binding drugs share the glutarimide ring, which is required for interactions with key residues in CRBN (18, 19) (Figure 1a). Treatment of cells with excess glutarimide reduces the effects of IMiDs through competition for this binding pocket, although the effect is weak due the low affinity of glutarimide for CRBN in the absence of the pthaloyl ring (18, 30).

Plant hormones work via induced degradation of target proteins

In plants, almost all aspects of growth and development are regulated by small molecules known as phytohormones. Numerous classes of phytohormones have been described, including absicic acid, auxin, brassinosteroid, cytokinin, ethylene, gibberellic acid, jasmonate, salicylic acid, and strigolactone. Phytohormones can act as either paracrine or endocrine signals to control essential organismal functions such as organ development, immune defense, and environmental response (20, 31-33).

Protein degradation through the ubiquitin-proteasome system has been implicated in the function of all phytohormones, which primarily target transcription factors for degradation. The *Arabidopsis* genome encodes over 1,500 E3 ubiquitin ligases, and Cullin-RING ligases in

particular play a central role in hormone signaling. Three classes of phytohormones—auxin, jasmonate, and gibberellic acid—directly control E3 ligase-substrate interaction (20, 31-33).

The best understood of these is auxin, which binds to the TIR1 ubiquitin ligase and induces the recruitment of target proteins containing the AUX/IAA degron (16, 34, 35). Structural evidence demonstrates that auxin binds at the interface between TIR1 and AUX/IAA without inducing significant conformational changes in either partner. Instead, auxin fills a hydrophobic cavity at the interaction surface, acting as a "molecular glue" to promote the TIR1-AUX/IAA interaction (16). Jasmonate regulates the interaction between the COI1 E3 ubiquitin ligase and JAZ proteins through a similar mechanism (17).

Approach

We sought to identify a cell line with endogenous production of a lenalidomide-like activity which induces degradation of the IKZF3 degron. Since IKZF1 and IKZF3 are essential in B and T cell development, we hypothesized that "endogenous lenalidomide" (eLen) might be involved in immune cell development and the coordination of the immune response throughout an organism. In order to identify a cell line with eLen activity, we tested hematopoietic cell lines for a number of criteria: (i) Proteasomal degradation of IKZF1 in the absence of lenalidomide, (ii) Increased post-translational stability of an IKZF3 reporter following treatment with glutarimide, a small-molecule which competes with lenalidomide for binding to CRBN but does not affect the post-translational stability of IKZF1, IKZF3, or CK1α, (iii) Ability of metabolites extracted from that cell line to decrease the stability of an IKZF3 post-translational stability reporter expressed in a non-hematopoietic HEK 293T reporter cell line. Through these assays, we identified a T-cell acute lymphoblastic leukemia (T-ALL) cell line, Molt-4, which satisfies all three criteria. Subsequent efforts were aimed at biochemical characterization of this eLen

activity. We ultimately sought a more unbiased approach to identify a source of eLen with a clear genetic trigger, which will hopefully prove useful for further identification efforts.

Methods

Reagents

Lenalidomide (Toronto Research Chemicals and Selleck Chemicals), Pomalidomide (Selleck Chemicals), MG-132 (Selleck Chemicals and EMD Millipore), Glutarimide (Sigma), and Epoxomicin (ApexBio) were dissolved in DMSO at 10 to 100 mM and stored at -80°C. For cell culture experiments final DMSO concentration was 0.1% or lower.

Cell lines

Cell lines listed in Table 1 were acquired from the Broad Institute. 293T cells were from ATCC. PRISM cell line pools were provided by the PRISM project at the Broad Institute. Cells were cultured in RPMI 1640 (GenClone) or DMEM (GenClone) supplemented with 10% heat-inactivated fetal bovine serum (FBS) (Omega Scientific) and 1% penicillin, streptomycin, and L-glutamine (Caisson). Cells were grown at 37˚C in a humidified incubator with 5% CO_2.

Western blot and antibodies

Protein lysates were run on Tris-HCl 1mm Criterion Precast gels (Bio-Rad) gels at a constant voltage. Proteins were transferred onto Immobilon-P transfer membranes (Millipore) at a constant amperage. Blots were blocked in 5% non-fat dry milk (Santa Cruz) or 5% BSA in TBS-T 0.1% for 30 minutes.

For protein detection primary antibodies detecting FLAG (M2, HRP-conjugate Sigma Aldrich), Actin (HRP-conjugate, Abcam), IKZF1 (H100, Santa Cruz Biotechnology), and IKZF3

(Imgenex). Secondary antibodies were HRP conjugated Bovine anti-Goat (Jackson ImmunoResearch) and HRP conjugated donkey anti-rabbit (GE Healthcare, Prometheus). SuperSignal (Thermo Scientific) chemiluminescent substrate was used for detection. For re-probing, blots were stripped in Restore Western Blot Stripping Buffer (Thermo Scientific), activated in methanol, and re-blocked. Western blot bands were quantitated with ImageJ when indicated.

Plasmids and virus constructs

The Artichoke constructs were as described in Sievers et al. (25) (Addgene #73320). Their structure is shown in Figure 2c and the amino acids included in the construct are listed below. Lentivirus was packaged using VSVG and pSpax2, as previously described (25). The FLAG-CRBN construct was previously described (22).

Construct	Amino acids included
IKZF3 degron	130-189
ZFP91	301-464
RNF166	24-237
ZNF692	318-481

Metabolite extraction

Metabolites were initially extracted according to Sellick et al. (36). Optimization was attempted with methods from Dietmair et al. (37), including a quench in either cold saline or the quench buffer described by Sellick et al. The method of eLen extraction used for large scale purification attempts was as follows: Molt-4 cells were grown in RPMI supplemented with 10% fetal bovine serum to confluence (approximately 2 million cells/mL). For large scale production, cells were grown in 3L Fernback flasks shaking at 60 rpm on an orbital shaker. The cell-media

mixture was quenched by rapid addition of 4x the volume of cold (0-4°C) saline (9g NaCl per L distilled water) and the mixture was centrifuged at 1000g for 1 minute. The supernatant was aspirated and 90°C ethanol or water was used to resuspend the pellet (2-8 mL per 2.5 million cells). Tubes were vortexed for 30 seconds and incubated at 90°C for 10 min. Tubes were then cooled on ice for 5 minutes and centrifuged for 5 minutes at 20,000g. The supernatant was filtered through a 2-3kD filter (Amion) in <70% ethanol for 30 minutes at 14,000g. The filtrate was dried down at room temperature overnight in a speedvac, sometimes after initial reduction of volume using a rotovap. Once dry, metabolites were manually resuspended in 1-10µL DMSO. 50 µL media per test well was added to this mixture. The media-metabolite mixture was added to 293T cells plated the day before treatment at 50,000 cells/well in 50 µL/well in a 96 well plate. Cells were incubated with metabolites for 4-6 hours before analysis by flow cytometry.

Flow cytometry

Flow cytometry was performed on a FACS LSRII (BD Bioscience) using a high throughput sampler (BD). Data were analyzed with FlowJo with gating on $mCherry^+$ cells.

Immunoprecipitation of CRBN

Molt-4 cells were infected with lentiviral vectors expressing FLAG-CRBN and the IZKF3 degron reporter. After selection with puromycin and expansion, cells were treated with DMSO or glutarimide, lysed in IP lysis buffer (Pierce) and incubated with anti-FLAG M2 Affinity Gel (Sigma-Aldrich) or anti-FLAG M2 magnetic beads (Sigma-Aldrich) for four hours at 4°C. Immunoprecipitates were washed three times in tris buffered saline (TBS) and eluted from the affinity gel with 250 µg/mL FLAG peptide (Sigma) after incubation for 30 min at 4°C. The resulting eluates were crashed in cold 80% methanol/20% water and filtered through a 2 kD

Filter (Vivacon, Sartorius). The filtrate was dried down in a Speedvac overnight, resuspended in DMSO, and applied to 293T reporter cells.

CRBN-DDB1 column

CRBN-DDB1 conjugated to CN BR sepharose beads (GE) was the kind gift of Eric Fischer (Dana Farber Cancer Institute). Briefly, the protocol was as follows: CRBN and DDB1 were produced in insect cells as previously described (19, 25, 26). CnBr was dissolved with 1 mM HCl, washed for 15 minutes on a sintered glass filter (porosity G3) with low pH washing solution (1M acetic acid/sodium acetate pH 4.0, 0.5 M NaCl). The CRBN-DDB1 solution was prepared in coupling buffer (0.1 M NaHCO3, 0.5 M NaCL, pH 8.3) with 3-13 mg of protein per 1 mg of swollen CnBr sepharose resin. The solution was incubated with the resin for 1 hr at room temperature with end-over-end rotation. After incubation, the resin was washed with five column volumes of coupling buffer and remaining active groups were blocked by incubation with 0.1 M Tris-HCl pH 8.0 for two hours. The resin was then washed with at least three cycles of alternating pH (at least 5 column volumes each) with 0.1 M acetic acid/sodium acetate pH 4.0 with 0.5 M NaCl and 0.1 M Tris-HCl pH 8.0, 0.5 M NaCl. The resin was sorted in a buffer containing 0.005% sodium azide.

To bind metabolites, CRBN-DDB1 resin was loaded onto a column. eLen was resuspended in TBS and bound to the column for 1 hr with end-over-end rotation at room temperature or 4°C. The column was washed three times in TBS and the protein was denatured and eLen eluted with methanol.

Time-resolved fluorescence resonance energy transfer

The TR-FRET assay was as described (25, 26) and used recombinant IKZF1 or CK1α and DDB1-CRBN. Activity was quenched with unlabeled wild-type CRBN, unlabeled CRBN IMiD-binding mutant (P352G W386A) or buffer (negative control). eLen used in this assay was HPLC fractionated.

In vitro *ubiquitination*

IKZF1 fluorescent ubiquitination was performed by mixing the biotinylated IKZF1 (isolated degron, Δ1-82, Δ198-239, Δ256-519, 0.5 μM), E3 (CRBN-DDB1-CUL4-RBX1, 0.1 μM), E2 (UbcH5a, 1 μM), E1 (UBA1, 0.05 μM), ubiquitin (10 μM), ubiquitin-fluorescin (0.2 μM), terbium-coupled streptavidin (2 nM) in the reaction buffer (B-71, Boston Biochem) supplemented with ATP (1 μM). After dispensing the assay mixture (15 μL volume), increasing concentration of lenalidomide or single concentration of cell extract was dispensed. The negative control was prepared by not including the E2 enzyme in the assay mixture.

After excitation of terbium fluorescence at 337 nm, emission at 490 nm (terbium) and 520 nm (fluorescin) were recorded with a 70 μs delay over 600 μs to reduce background fluorescence, and the reaction was followed over 60 cycles of each data point using a PHERAstar FS microplate reader (BMG Labtech). The TR-FRET signal of each data point was extracted by calculating the 520/490 nm ratio.

Solid phase extraction

Multiple solid phase extraction methods were evaluated using Waters Oasis and Phenomenex products. The optimized protocol involved HLB Prime columns (Waters). Samples were resuspended in water with 2% formic acid, loaded onto the columns and drawn through

using a vacuum manifold box. Samples were washed in water (1 mL for a 1 cc column) and samples were eluted with 90% acetonitrile/10% methanol and dried down in a speedvac overnight at room temperature.

High performance liquid chromatography-mass spectrometry (HPLC-MS)

Multiple HPLC methods were attempted using columns including Atlantis T3, Chiralpak AD-RH, Luna Phenyl Hexyl, Hydro, HILIC, and Gemini. The data shown here were generated on an Atlantis T3 column (100 Å, 3 μm, 3 x 150 mm). Figures 6a-b was generated using the following protocol: eLen was resuspended in 80% water, 20% acetonitrile, 0.08% formic acid and 0.02% acetic acid. The method was as follows with buffer A= H_20 + 0.01% Formic acid and buffer B= ACN + 0.01% Acetic acid. The percent buffer B is given. The percent buffer A was 100-percent buffer B.

Time (min)	%Buffer B	Flow (ml/min)
0	20	0.45
3	20	0.45
15	100	0.45
18	100	0.45
19	20	0.45
27	Stop	

Data shown in Figure 6c were generated with the following protocol. eLen was resuspended in 80% H_20 + 0.01% formic acid , 20% ACN +0.01% Acetic acid. The method was as follows with buffer A= H_20 + 0.01% Formic acid and buffer B= ACN + 0.01% Acetic acid. The percent buffer B is given. The percent buffer A was 100-percent buffer B.

Time (min)	%Buffer B	Flow (ml/min)
0	5	0.45
3	5	0.45
15	100	0.45
18	100	0.45
19	20	0.45
27	Stop	

Data shown in Figure 6d were generated with the following protocol. eLen was resuspended in 80% H_20 + 0.01% formic acid , 20% ACN +0.01% Acetic acid. Buffer A= 95% H_20 + 5% ACN with 10 mM ammonium formate, pH 3.5 and Buffer B=ACN. The method was as follows:

Time (min)	%Buffer B	Flow (mL/min)
0	0	0.8
25	0	0.8
35	10	0.8
40	100	0.8
45	0	0.8
55	0	0.8

Results

IKZF1 is endogenous degraded in T-ALL cell lines and is stabilized by treatment with glutarimide

We hypothesized that an endogenous lenalidomide-like activity might be present in hematopoietic cell lines. We were particularly interested in T acute lymphoblastic leukemia cell lines given a prior report (38) that a human T-ALL cell line, Molt-4, and a mouse thymocyte leukemia cell line, VL3-3M2, have endogenous ubiquitination and proteasomal degradation of IKZF1. To test whether hematopoietic cells endogenously degrade IKZF1 and IKZF3, we

obtained the cell lines shown in Table 1, which represent several different hematopoietic diseases.

We treated these cells with the proteasome inhibitors MG-132 and epoxomicin for 6 hours (Figure 2a-b). Treatment with proteasome inhibitors increased the stability of IKZF1 in Molt-4 and Reh cells. We infected these cells with the IKZF3-Artichoke reporter (25) (Figure 2c), which provides a measure of the post-translational stability of proteins based on the fluorescence of enhanced green fluorescent protein (eGFP) tagged with the IZKF3-IMiD degron compared to an untagged mCherry. Treatment with high doses of glutarimide increased the post-translational stability of the IZKF3 degron in Molt-4 and Jurkat T-ALL cells (Figure 2d). Glutarimide also increased the protein levels of endogenous IKZF1 in Molt-4 cells (Figure 2e). Taken together, these results suggest that endogenous IKZF1 and IKZF3 are degraded by the proteasome in T-ALL cell lines and this process can be blocked by competitive inhibition of the lenalidomide-binding pocket of CRBN.

Metabolite extracts from T-ALL cells can induce CRBN-dependent degradation of IKZF1 and IKZF3 in reporter cell lines

We next asked whether the endogenous IKZF1- and IKZF3-degrading activity of T-ALL cell lines might derive from a small molecule, rather than a post-translational modification or recruitment of an additional binding partner. We treated 293T reporter cell lines with conditioned media from T-ALL cell lines, but this did not induce degradation of the IKZF3 degron reporter (data not shown). Next, we extracted whole cell metabolites from Jurkat and Molt-4 cells (Figure 3a). After drying and resuspension in media, these metabolites induced the degradation of the IKZF3 degron reporter in 293T with wild-type CRBN, but not 293T cells with biallelic disruption of CRBN via CRISPR Cas9 genome editing (25)(CRBN KO, Figure S1). Similarly,

the extracted metabolites did not induce significant degradation of an IKZF3-Q147H mutant reporter which disrupts recognition of the IKZF3 degron by CRBN (13). Similar results were seen with a reporter containing full length IKZF3 (Figure 3b). The observed IKZF3-degrading activity was not affected by treatment with Proteinase K, consistent with activity due to a metabolite rather than a protein or peptide (Figure 3c). These results suggest that T-ALL cells contain an extractable intracellular metabolite that induce CRBN-dependent degradation of the IKZF3-degron. We hereafter refer to this activity as endogenous lenalidomide (eLen).

IKZF1 and IKZF3-degrading activity immunoprecipitates with CRBN and can induce ubiquitination and degradation of IZKF1 **in vitro**

If there exists an endogenous metabolite that acts as a molecular glue between CRBN and IKZF1/IKZF3, we hypothesized that we could recover this activity through immunoprecipitation of CRBN in cells expressing IKZF3.

We expressed FLAG-CRBN and the IKZF3 degron in Molt-4 cells (Figure 3d). We immunoprecipitated CRBN from these cells with anti-FLAG beads, denatured the immunoprecipitates with methanol, and filtered through a 2 kDa filter to remove residual protein. The resulting metabolites induced CRBN-dependent degradation of the IKZF3 reporter in 293T cells, which was not seen in with bead-only mock immunoprecipitates (Figure 3e). Treatment of the cells with glutarimide before and during immunoprecipitation decreased the amount of eLen activity recovered, as expected if glutarimide is a competitive binding inhibitor of eLen.

Similarly, whole cell metabolite extracts were applied to a column containing recombinant CRBN-DDB1 resin (Figure 3f). eLen activity bound to this column through three washes, with the majority of activity eluting once the CRBN-DDB1 complexes were denatured

with methanol (Figure 3g). These data again suggest that eLen has direct affinity for CRBN-DDB1.

We next asked whether the extracted eLen could induce the recruitment of IMiD-induced substrates to CRBN *in vitro.* To evaluate this, we used a time-resolved fluorescence resonance energy transfer assay (26) diagrammed in Figure 4a. We observed that eLen induced recruitment of IKZF1 to CRBN as shown by an increase in the A530/A490 ratio (Figure 4b). This effect was blocked by the addition of excess untagged wild-type CRBN but not by the addition of untagged mutant CRBN that is unable to bind IMiDs, suggesting that eLen exerts its action through the IMiD binding site. Similar results were observed with CK1α (Figure 4c). Furthermore, eLen increased the ubiquitination of IKZF1 in a fluorescence-based assay (Figure 4d). Taken together, these results demonstrate that eLen induces the recruitment of IZKF1 and CK1α to CRBN and enhances their ubiquitination by $CRL4^{CRBN}$.

Endogenous IKZF3-degrading activity can be recovered and purified using biochemical methods

We sought to use biochemical fractionation methods and high performance liquid chromatography-mass spectrometry (HPLC-MS) to identify the m/z ratio and chemical structure of eLen. Since these methods require large input amounts, we first optimized extraction of eLen activity from Molt-4 cells. Comparison of a number of published methods (36, 37) for the extraction of metabolites from cell lines suggested that methods involving freezing, which had previously been used, decreased the extraction of eLen activity (Figure 5a). Freezing after extraction also significantly decreased eLen activity (Figure 5b). Subsequent work was conducted using hot ethanol or water extraction of eLen and extraction efficiency was dependent on solvent volume (Figure 5c).

We used solid phase extraction (SPE) to broadly fractionate eLen activity before high performance liquid chromatography. Multiple sorbents were tested, include Oasis and Phenomenex products (data not shown). eLen activity was best-retained on an HLB Prime column (Figure 5d), with maximal elution in 22.5% acetonitrile, 2.5% methanol and 75% water (Figure 5e).

SPE-purified eLen was used to develop a number of HPLC-based purification methods. eLen from whole cell extracts and CRBN immunoprecipitation had identical retention times, again suggesting that both extraction methods capture the same molecule (Figure 6a). A small change in the starting organic solvent concentration led to a large shift in the retention time of eLen activity, allowing comparison of the m/z ratios observed in the active peak of two different protocols (Figure 6b-c). Some HPLC methods produced peaks of eLen activity at two different retention times, although repeat chromatography of the active fractions demonstrated conversion from a long-retention form to a short-retention form consistent with interconversion between two forms or a parent molecule and active degradation product (Figure 6d).

There was significant loss of activity throughout the purification and no UV signature or m/z ratio could be found that correlated with activity, consistent with eLen's poor stability. A targeted search for the m/z ratio of lenalidomide (260.103) identified this m/z at the limit of detection in the active fractions from some runs, raising concern that the activity observed could be due to lenalidomide contamination. However, eLen activity was still observed when the extraction protocol was performed by a contract research organization (Figure 6e). Ultimately, the identification of the m/z responsible for the eLen activity observed will require the ability to increase the production and stability of the endogenous activity.

Endogenous degradation of other IMiD protein targets

Given recent findings regarding the differing substrate specificities of IMiD derivatives, we asked whether the eLen might also induce the degradation of additional proteins recently identified as IMiD targets (25, 39). Using Artichoke flow-cytometry based post-translational protein stability reporters, we found that Molt-4 cell extracts induced degradation of ZNF692 and RNF166 in a CRBN-dependent manner (Figure 7a).

ZNF692 and RNF166 are more strongly degraded by pomalidomide than lenalidomide (25, 39). We wondered whether Molt-4-extract-induced degradation of IKZF3, ZNF692, and RNF166 could result from different compounds within the complex cellular extract. To evaluate this, we began with solid phase extraction of the Molt-4 extract and measured the relative activity of each fraction in the three different reporter systems (Figure 7b). These data suggested subtle differences in the distribution of activity among the fractions, with RNF166 and ZNF692-degrading activity primarily in the flow through and the IKZF3-degrading activity split between flow through and elution. This suggested that the zinc finger-degrading activities present in Molt-4 cell extract might be due to multiple compounds that differ in their relative polarity. This hypothesis was further supported by the analysis of HPLC fractions (Figure 7c-e), which showed a distinct pattern of degrading activity for the IKZF3 and RNF166 reporters. These data are consistent with either activity due to multiple distinct compounds present in Molt-4 cellular extracts or different substrate specificities of the long and short retention forms of eLen observed on HPLC, which may represent structural interconversion or degradation of a parent molecule (Figure 6d). However, further confirmation of these findings awaits the identification of the chemical structure of eLen and RNF166 and ZNF692-degrading activities.

Screen of cell line pools to identify additional cell lines producing eLen

Given difficulties with producing sufficient quantities of stable eLen, we sought to identify additional cell lines with eLen activity, again using increased IKZF3 post-translational stability following glutarimide treatment as a proxy for endogenous degradation mediated through CRBN's IMiD-binding pocket. To approach this question in an unbiased manner we took advantage of the pools of tumor cell lines created by the PRISM project (40) and adapted to grow together. We obtained 27 pools of suspension cell lines (average 5 cell lines/pool) and infected these cell pools with the IKZF3 degron reporter (Figure 8a). Following infection, we treated the pools with glutarimide and analyzed the mean fluorescence intensity of GFP/mCherry in pooled infected cells. An initial screen identified four cell pools with GFP/mCherry ratios >1 following treatment with both 10 μM and 100 μM glutarimide. Initial cell line pool hits (Supplementary Fig S2) were re-screened with both the wild-type and IKZF3 Q147H reporter, although one pool could not be recovered. For the three remaining pools, glutarimide treatment resulted in an increase in the GFP/mCherry ratio of the wild-type IKZF3 reporter but not the Q147H IKZF3 mutant reporter, suggesting endogenous degradation of the degron region of IKZF3 which depends on similar structural integrity of the zinc finger as is required for lenalidomide-induced degradation. Of the three re-tested pools, we noted that one of the pools contained a rhabdoid cancer cell line, BT-12, and another contained Peds005T Susp, a novel renal medullary carcinoma cell line (41). Both rhabdoid tumors and renal medullary carcinomas depend on loss of the tumor suppressor SMARCB1 (42), a core member of the SWI/SNF complex that is frequently disrupted in human cancer. Given the availability of inducible SMARCB1 re-expression models, we pursued the Peds005TSusp cell line as another potential source of eLen.

Peds005TSusp cells have endogenous CRBN-dependent degradation of the IKZF3 degron and produce eLen

We confirmed that glutarimide treatment increased the post-translational stability of the IKZF3 degron, but not a similar zinc finger, ZFP91, in Peds005TSusp cell line (Figure 8d-e). This correlated with endogenous proteasomal degradation of the IZKF3 degron, but not ZFP91, in the Peds005TSusp cell line (Figure 8f). At least some of this degradation occurred through CRBN, as CRISPR-Cas9 mediated gene editing of CRBN resulted in an increase in the post-translational stability of the IKZF3 degron reporter in cells infected with gRNA targeting CRBN but not non-targeting guides (Figure 8g). A statistically-significant increase in the post-translational stability of the IKZF3 degron reporter with CRBN knockout was not seen following treatment with glutarimide, as expected if glutarimide stabilizes endogenous IKZF3 by competitively inhibiting its interaction with CRBN. As in Molt-4 cells, this endogenous and glutarimide-sensitive proteasomal degradation of the IKZF3 degron was associated with the presence of extractable metabolites which induced CRBN-dependent degradation of the IKZF3 degron in 293T reporter cells (Figure 8h).

Peds005TSusp cells are dependent on heterozygous loss of SMARCB1 and enforced expression of SMARCB1 results in cellular senescence (41). Thus, we asked whether the endogenous degradation of the IZKF3 degron is dependent on inactivation of SMARCB1. We obtained Peds005TSusp cells expressing a doxycycline-inducible SMARB1 expression construct (kind gift of A. Hong) and infected these cells with the IKZF3 degron reporter. Expression of SMARCB1 in Ped005TSusp cells increased the post-translational stability of the IKZF3 degron, but this effect was not seen when cells were also treated with glutarimide, consistent with a CRBN-mediated effect (Figure 8i). Taken together, these results suggest that loss of SMARCB1

creates a cellular state associated with increased proteasomal degradation of the IKZF3 degron through CRBN.

Discussion, Conclusions, and Suggestions for Future Work

This work identified cell lines that produce an extractable small molecule that can induce the ubiquitination and degradation of the lenalidomide-responsive region of IZKF3 in a CRBN-dependent manner. Although structural details of the eLen-CRBN interaction remain to be determined, several pieces of evidence suggest that this molecule depends on the same structural motifs in IZKF3 as lenalidomide and functions to recruit IZKF1 and CK1α to CRBN, consistent with the "molecular glue" mechanism common to both lenalidomide and plant hormones.

Unfortunately, this work was unable to identify the endogenously produced compound responsible for CRBN-dependent IZKF3 degradation, for which there are several potential explanations. It remains formally possible that the CRBN-dependent degradation of IKZF3 observed in reporter cells is driven by a factor other than an endogenous metabolite produced by Molt-4 or Peds005TSusp cells. For example, metabolite extracts could trigger state changes in 293T reporter cells which result in degradation of the IKZF3 degron through a post-translational modification. Alternatively, Molt-4 cells could produce an endogenous compound that alters the fluorescence of mCherry or GFP. However, these explanations are unlikely given that the effect is dependent on CRBN, is not observed with similar GFP/mCherry reporters with a mutant IKZF3 degron, and persists after metabolite purification by SPE and HPLC. Additionally, the metabolite extracts can be isolated via affinity purification with CRBN and induce interactions between IZKF1, CK1α, and CRBN in fully *in vitro* systems, suggesting a directly-interacting small molecule rather than a post-translational modification.

The most likely explanation for the failure of compound identification by mass spectrometry is a mismatch between the sensitivity of the flow-cytometry-based IKZF3 reporter system and biochemical methods, coupled with poor stability of an endogenous metabolite. The IKZF3-Artichoke reporter has picomolar sensitivity but identification of an unknown by HPLC-MS requires greater quantities of the active compound, which was limited by the need for cellular extracts. Successful biochemical purification often require large volumes of input material, as in the identification of the most common form of auxin, 3-indole acetic acid (IAA), from human urine (43). Multiple studies with eLen also demonstrated that the endogenous activity is unstable over time, further complicating our ability to generate the large amount of activity required for biochemical purification through sequential steps. Additionally, the ability to distinguish the active compound from the many inactive compounds in a complex cellular extract is limited by the lack of clear trigger for eLen production in the tested cell lines.

Contamination with known IMiD compounds provides another explanation for these results. However, while lenalidomide was detected in some MS samples, activity persisted with compound was produced by a CRO without prior IMiD work. Additionally, the extracted metabolites seem to have a slightly different pattern of activity than lenalidomide, with more potent degradation of RNF166 and ZNF692 relative to IKZF3 than is seen with lenalidomide. Overall, it is difficult to reconcile the multiple independent lines of evidence implicating Molt-4 and Peds005TSusp cells, including endogenous proteasomal degradation of IKZF1 which is blocked by glutarimide and the effects of CRBN knockout and SMARCB1 re-expression, with contamination by lenalidomide.

If we were to continue to pursue a biochemical fractionation approach, the next steps to identify the chemical structure of eLen would be to scale up extract production, identify an m/z

ratio by HPLC-MS, and use nuclear magnetic resonance to further delineate the chemical structure. However, it is unclear if we will be able to generate the large amount of pure material required for this approach using cellular extracts. Hopefully, technical advances in HPLC-MS will enable identification of an m/z with lower amounts of activity. Alternatively, crystallization of the CRBN-eLen-IKZF1/3 complex may be possible at lower eLen concentrations, which would help to both further delineate eLen's chemical structure and biochemical mechanism.

Another potential approach would be to try to determine the metabolic pathways controlling eLen production in order to gain insight into both its regulation and metabolic pathway, which may in turn shed light on its chemical structure. While induction of SMARCB1 has some effect on eLen production, the effect size is small and it is unclear whether this effect is specific or is related to the induction of cellular senescence. Ideally, we would want to identify a single perturbation that induces large changes in eLen production. While such a perturbation may provide insight into the metabolic or cellular pathways involved in eLen production, it would also provide an essential comparator in biochemical fractionation and could potentially allow us to more easily identify the active metabolite by comparing the relative abundances of each m/z ratio present in extracts from perturbed and un-perturbed cells.

A genome-wide screen is one unbiased approach to determine which metabolic and cellular pathways might influence eLen production. An open-reading-frame (ORF)-overexpression screen (44) provides the opportunity to enhance the activity of specific metabolic pathways which may be involved in eLen production, and thus potentially increase eLen activity yields. Such a screen could be conducted in $CRBN^{+/+}$ and $CRBN^{-/-}$ cells expressing the IZKF3-wild-type or IZKF3 Q147H reporter, thus limiting hits to ORFs that alter CRBN-dependent degradation of the lenalidomide-responsive region of IKZF3.

The cellular system reported here may represent the first example of an endogenous compound in mammalian cells that regulates transcription factors through induced recruitment to E3 ligases and subsequent ubiquitination and degradation. If small-molecule regulation of E3 ubiquitin ligases can be confirmed in human cells, it will provide essential insight into the regulation of protein levels in both health and disease. Understanding endogenous regulatory mechanisms may also enable pharmacological modulation of ubiquitin ligase activity for novel substrates, ligases, and clinical conditions. Additionally, mimics of endogenous compounds may provide fruitful areas for novel drug development and may be especially suited to degrade transcription factors, which have proved challenging drug targets.

Summary:

This thesis sought to identify an endogenous metabolite in human cells that binds to the E3 ubiquitin ligase CRBN and induces the recruitment and ubiquitination of the lymphoid transcription factor IKZF3, analogous to the mechanism of thalidomide derivatives. This would represent a completely novel mechanism of regulation in mammalian cells, but is analogous to several important classes of plant hormones. Several cellular contexts were identified in which IZKF1 and IZKF3 are degraded by the proteasome. Degradation was reduced by treatment with glutarimide, a small molecule competitive inhibitor of the CRBN IMiD-binding pocket. Metabolites extracted from these cell lines induced CRBN-dependent degradation of IKZF3 in reporter cell lines, suggesting activity due to a small molecule rather than a post-translational modification. Several biochemical assays confirmed direct interaction between the metabolites and CRBN and extracted metabolites induced the recruitment and ubiquitination of IKZF1 *in vitro*. Extracted metabolites also induced the degradation of additional recently described IMiD substrates. Extraction and purification methods were developed to isolate this activity, dubbed

eLen. Although HPLC-MS identification of an m/z ratio was ultimately unsuccessful due to low input amounts and poor stability of the compound, it is hoped that technological develops in mass spectrometry will allow identification of this activity in the future. Finally, an unbiased screen of cell lines was undertaken to identify additional cellular contexts in which this activity could be identified, providing an avenue for further study.

References:

1. Fink EC, Ebert BL. The novel mechanism of lenalidomide activity. Blood. 2015;126(21):2366-9. Epub 2015/10/07. doi: 10.1182/blood-2015-07-567958. PubMed PMID: 26438514; PubMed Central PMCID: PMCPmc4653765.

2. Attal M, Lauwers-Cances V, Marit G, Caillot D, Moreau P, Facon T, et al. Lenalidomide maintenance after stem-cell transplantation for multiple myeloma. The New England journal of medicine. 2012;366(19):1782-91. doi: 10.1056/NEJMoa1114138.

3. McCarthy P, Owzar K, Hofmeister C, Hurd D, Hassoun H, Richardson P, et al. Lenalidomide after stem-cell transplantation for multiple myeloma. The New England journal of medicine. 2012;366(19):1770-81. doi: 10.1056/NEJMoa1114083.

4. Palumbo A, Hajek R, Delforge M, Kropff M, Petrucci M, Catalano J, et al. Continuous lenalidomide treatment for newly diagnosed multiple myeloma. The New England journal of medicine. 2012;366(19):1759-69. doi: 10.1056/NEJMoa1112704.

5. Weber D, Chen C, Niesvizky R, Wang M, Belch A, Stadtmauer E, et al. Lenalidomide plus dexamethasone for relapsed multiple myeloma in North America. The New England journal of medicine. 2007;357(21):2133-42. doi: 10.1056/NEJMoa070596.

6. Rajkumar S, Hayman S, Lacy M, Dispenzieri A, Geyer S, Kabat B, et al. Combination therapy with lenalidomide plus dexamethasone (Rev/Dex) for newly diagnosed myeloma. Blood. 2005;106(13):4050-3. doi: 10.1182/blood-2005-07-2817.

7. Habermann TM, Lossos IS, Justice G, Vose JM, Wiernik PH, McBride K, et al. Lenalidomide oral monotherapy produces a high response rate in patients with relapsed or refractory mantle cell lymphoma. British journal of haematology. 2009;145(3):344-9. doi: 10.1111/j.1365-2141.2009.07626.x.

8. Chanan-Khan A, Miller KC, Musial L, Lawrence D, Padmanabhan S, Takeshita K, et al. Clinical efficacy of lenalidomide in patients with relapsed or refractory chronic lymphocytic leukemia: results of a phase II study. Journal of clinical oncology : official journal of the American Society of Clinical Oncology. 2006;24(34):5343-9. doi: 10.1200/JCO.2005.05.0401.

9. Ferrajoli A, Lee B-NN, Schlette EJ, O'Brien SM, Gao H, Wen S, et al. Lenalidomide induces complete and partial remissions in patients with relapsed and refractory chronic lymphocytic leukemia. Blood. 2008;111(11):5291-7. doi: 10.1182/blood-2007-12-130120.

10. List A, Dewald G, Bennett J, Giagounidis A, Raza A, Feldman E, et al. Lenalidomide in the myelodysplastic syndrome with chromosome 5q deletion. The New England journal of medicine. 2006;355(14):1456-65. doi: 10.1056/NEJMoa061292.

11. List A, Kurtin S, Roe D, Buresh A, Mahadevan D, Fuchs D, et al. Efficacy of lenalidomide in myelodysplastic syndromes. The New England journal of medicine. 2005;352(6):549-57. doi: 10.1056/NEJMoa041668.

12. Fenaux P, Giagounidis A, Selleslag D, Beyne-Rauzy O, Mufti G, Mittelman M, et al. A randomized phase 3 study of lenalidomide versus placebo in RBC transfusion-dependent patients with Low-/Intermediate-1-risk myelodysplastic syndromes with del5q. Blood. 2011;118(14):3765-76. doi: 10.1182/blood-2011-01-330126.

13. Krönke J, Udeshi ND, Narla A, Grauman P, Hurst SN, McConkey M, et al. Lenalidomide causes selective degradation of IKZF1 and IKZF3 in multiple myeloma cells. Science (New York, NY). 2014;343(6168):301-5. doi: 10.1126/science.1244851.

14. Gandhi AK, Kang J, Havens CG, Conklin T, Ning Y, Wu L, et al. Immunomodulatory agents lenalidomide and pomalidomide co-stimulate T cells by inducing degradation of T cell

repressors Ikaros and Aiolos via modulation of the E3 ubiquitin ligase complex CRL4(CRBN.). British journal of haematology. 2014;164(6):811-21. doi: 10.1111/bjh.12708.

15. Lu G, Middleton RE, Sun H, Naniong M, Ott CJ, Mitsiades CS, et al. The myeloma drug lenalidomide promotes the cereblon-dependent destruction of Ikaros proteins. Science (New York, NY). 2014;343(6168):305-9. doi: 10.1126/science.1244917.

16. Tan X, Calderon-Villalobos LI, Sharon M, Zheng C, Robinson CV, Estelle M, et al. Mechanism of auxin perception by the TIR1 ubiquitin ligase. Nature. 2007;446(7136):640-5. doi: 10.1038/nature05731.

17. Sheard LB, Tan X, Mao H, Withers J, Ben-Nissan G, Hinds TR, et al. Jasmonate perception by inositol-phosphate-potentiated COI1-JAZ co-receptor. Nature. 2010;468(7322):400-5. doi: 10.1038/nature09430.

18. Chamberlain PP, Lopez-Girona A, Miller K, Carmel G, Pagarigan B, Chie-Leon B, et al. Structure of the human Cereblon-DDB1-lenalidomide complex reveals basis for responsiveness to thalidomide analogs. Nature structural & molecular biology. 2014;21(9):803-9. doi: 10.1038/nsmb.2874.

19. Fischer ES, Böhm K, Lydeard JR, Yang H, Stadler MB, Cavadini S, et al. Structure of the DDB1-CRBN E3 ubiquitin ligase in complex with thalidomide. Nature. 2014;512(7512):49-53. doi: 10.1038/nature13527.

20. Kelley DR, Estelle M. Ubiquitin-mediated control of plant hormone signaling. Plant Physiol. 2012;160(1):47-55. doi: 10.1104/pp.112.200527. PubMed PMID: 22723083; PubMed Central PMCID: PMCPMC3440220.

21. Ito T, Ando H, Suzuki T, Ogura T, Hotta K, Imamura Y, et al. Identification of a primary target of thalidomide teratogenicity. Science (New York, NY). 2010;327(5971):1345-50. doi: 10.1126/science.1177319.

22. Krönke J, Fink EC, Hollenbach PW, MacBeth KJ, Hurst SN, Udeshi ND, et al. Lenalidomide induces ubiquitination and degradation of casein kinase 1A1 in del(5q) MDS. Nature. 2015;523(7559):183-8. Epub 1 July 2015. doi: 10.1038/nature14610.

23. Boultwood J, Fidler C, Strickson A, Watkins F, Gama S, Kearney L, et al. Narrowing and genomic annotation of the commonly deleted region of the 5q- syndrome. Blood. 2002;99(12):4638-41. doi: 10.1182/blood.V99.12.4638.

24. Boultwood J, Pellagatti A, Cattan H, Lawrie C, Giagounidis A, Malcovati L, et al. Gene expression profiling of CD34+ cells in patients with the 5q- syndrome. British journal of haematology. 2007;139(4):578-89. doi: 10.1111/j.1365-2141.2007.06833.x.

25. Sievers QL, Petzold G, Bunker RD, Renneville A, Slabicki M, Liddicoat BJ, et al. Defining the human C2H2 zinc finger degrome targeted by thalidomide analogs through CRBN. Science. 2018;362(6414). doi: 10.1126/science.aat0572. PubMed PMID: 30385546; PubMed Central PMCID: PMCPMC6326779.

26. Petzold G, Fischer ES, Thoma NH. Structural basis of lenalidomide-induced CK1alpha degradation by the CRL4(CRBN) ubiquitin ligase. Nature. 2016;532(7597):127-30. Epub 2016/02/26. doi: 10.1038/nature16979. PubMed PMID: 26909574.

27. Matyskiela ME, Zhang W, Man H-WW, Muller G, Khambatta G, Baculi F, et al. A Cereblon Modulator (CC-220) with Improved Degradation of Ikaros and Aiolos. Journal of medicinal chemistry. 2018;61(2):535-42. doi: 10.1021/acs.jmedchem.6b01921.

28. An J, Ponthier CM, Sack R, Seebacher J, Stadler MB, Donovan KA, et al. pSILAC mass spectrometry reveals ZFP91 as IMiD-dependent substrate of the CRL4(CRBN) ubiquitin ligase. Nat Commun. 2017;8:15398. doi: 10.1038/ncomms15398. PubMed PMID: 28530236; PubMed Central PMCID: PMCPMC5458144.

29. Matyskiela ME, Lu G, Ito T, Pagarigan B, Lu CC, Miller K, et al. A novel cereblon modulator recruits GSPT1 to the CRL4(CRBN) ubiquitin ligase. Nature. 2016;535(7611):252-7. doi: 10.1038/nature18611. PubMed PMID: 27338790.

30. Lopez-Girona A, Mendy D, Ito T, Miller K, Gandhi AK, Kang J, et al. Cereblon is a direct protein target for immunomodulatory and antiproliferative activities of lenalidomide and pomalidomide. Leukemia. 2012;26(11):2326-35. doi: 10.1038/leu.2012.119. PubMed PMID: 22552008; PubMed Central PMCID: PMCPMC3496085.

31. Kelley DR. E3 Ubiquitin Ligases: Key Regulators of Hormone Signaling in Plants. Molecular & cellular proteomics : MCP. 2018;17(6):1047-54. doi: 10.1074/mcp.MR117.000476. PubMed PMID: 29514858; PubMed Central PMCID: PMCPMC5986243.

32. Santner A, Estelle M. The ubiquitin-proteasome system regulates plant hormone signaling. Plant J. 2010;61(6):1029-40. doi: 10.1111/j.1365-313X.2010.04112.x. PubMed PMID: 20409276; PubMed Central PMCID: PMCPMC3066055.

33. Shabek N, Zheng N. Plant ubiquitin ligases as signaling hubs. Nat Struct Mol Biol. 2014;21(4):293-6. doi: 10.1038/nsmb.2804. PubMed PMID: 24699076.

34. Dharmasiri N, Dharmasiri S, Estelle M. The F-box protein TIR1 is an auxin receptor. Nature. 2005;435(7041):441-5. doi: 10.1038/nature03543.

35. Kepinski S, Leyser O. The Arabidopsis F-box protein TIR1 is an auxin receptor. Nature. 2005;435(7041):446-51. doi: 10.1038/nature03542.

36. Sellick CA, Hansen R, Stephens GM, Goodacre R, Dickson AJ. Metabolite extraction from suspension-cultured mammalian cells for global metabolite profiling. Nature protocols. 2011;6(8):1241-9. doi: 10.1038/nprot.2011.366. PubMed PMID: 21799492.

37. Dietmair S, Timmins NE, Gray PP, Nielsen LK, Kromer JO. Towards quantitative metabolomics of mammalian cells: development of a metabolite extraction protocol. Anal Biochem. 2010;404(2):155-64. doi: 10.1016/j.ab.2010.04.031. PubMed PMID: 20435011.

38. Popescu M, Gurel Z, Ronni T, Song C, Hung KY, Payne KJ, et al. Ikaros stability and pericentromeric localization are regulated by protein phosphatase 1. The Journal of biological chemistry. 2009;284(20):13869-80. doi: 10.1074/jbc.M900209200.

39. Donovan KA, An J, Nowak RP, Yuan JC, Fink EC, Berry BC, et al. Thalidomide promotes degradation of SALL4, a transcription factor implicated in Duane Radial Ray syndrome. Elife. 2018;7. doi: 10.7554/eLife.38430. PubMed PMID: 30067223; PubMed Central PMCID: PMCPMC6156078.

40. Yu C, Mannan AM, Yvone GM, Ross KN, Zhang YL, Marton MA, et al. High-throughput identification of genotype-specific cancer vulnerabilities in mixtures of barcoded tumor cell lines. Nat Biotechnol. 2016;34(4):419-23. doi: 10.1038/nbt.3460. PubMed PMID: 26928769; PubMed Central PMCID: PMCPMC5508574.

41. Hong AL, Tseng YY, Wala JA, Kim WJ, Kynnap BD, Doshi MB, et al. Renal medullary carcinomas depend upon SMARCB1 loss and are sensitive to proteasome inhibition. Elife. 2019;8. doi: 10.7554/eLife.44161. PubMed PMID: 30860482; PubMed Central PMCID: PMCPMC6436895.

42. Roberts CW, Biegel JA. The role of SMARCB1/INI1 in development of rhabdoid tumor. Cancer Biol Ther. 2009;8(5):412-6. doi: 10.4161/cbt.8.5.8019. PubMed PMID: 19305156; PubMed Central PMCID: PMCPMC2709499.

43. Wieland OP, De Ropp RS, Avener J. Identity of auxin in normal urine. Nature. 1954;173(4408):776-7. doi: 10.1038/173776a0. PubMed PMID: 13165644.

44. Yang X, Boehm JS, Yang X, Salehi-Ashtiani K, Hao T, Shen Y, et al. A public genome-scale lentiviral expression library of human ORFs. Nature methods. 2011;8(8):659-61. doi: 10.1038/nmeth.1638. PubMed PMID: 21706014; PubMed Central PMCID: PMCPMC3234135.

Tables and Figures:

Figure 1: IMiDs and CRL4^{CRBN}. a, Chemical structures of thalidomide, lenalidomide, pomalidomide and glutarimide with the glutarimide and pthaloyl rings of the IMiDs indicated. **b**, Diagram of the CRL4^{CRBN} complex bound to lenalidomide and inducing the recruitment and ubiquitination of IKZF1.

Table 1

Disease	Cell Line
B-Acute Lymphoblastic Leukemia	
	RS4;11
	697
	Reh
T-Acute Lymphoblastic Leukemia	
	Molt-4
	Jurkat
B Lymphoma	
	RI-1
	MC116
Acute Myeloid Leukemia	
	KG-1
	Nomo-1
	HL-60
Monocytic	
	THP-1

Figure 2: Proteasomal degradation of IKZF1 in T-ALL cells is blocked by treatment with CRBN-binder glutarimide. a, The indicated cell lines were treated with DMSO (D), 10 μM glutarimide (G), 2 μM epoxomicin (E), 10 μM MG-132 (M), or 10 μM lenalidomide (L) for 6 hours, followed by immunoblotting for IKZF1, IKZF3, and actin as a loading control. The relative area of the IKZF1 band to the actin band in the same lane is quantitated in **b**. **c,** Diagram of the Artichoke IKZF3-degron post-translational stability reporter, which contains a 60 amino

acid region of IKZF3 that is sufficient for IMiD-induced degradation fused to enhanced green fluorescence protein (eGFP). An internal ribosome entry site (IRES) separates this fusion construct from mCherry, which is used as a normalization control. A decrease in the GFP/mCherry ratio indicates a decrease in the post-translational stability of the fused protein. **d**, The indicated cell lines were infected with the reporter shown in **c**. Cells were treated with DMSO, 10 μM glutarimide, 100 μM glutarimide, or 1 μM lenalidomide for 24 hours. Data are reported relative to the DMSO condition for each cell line. T cell acute lymphoblastic leukemia cell lines (T-ALL) are indicated. **e,** Immunoblot of endogenous IKZF1, IKZF3, and Actin in Molt-4 cells treated with DMSO (D) or Glutarimide 100 μM (G) for 24 hours.

Figure 3: Molt-4 cells contain metabolites that bind CRBN and induce CRBN-dependent degradation of the IKZF3 degron in reporter cells. a, Whole cell extracts were isolated from Jurkat or Molt-4 cells, dried down and applied to $CRBN^{+/+}$ or $CRBN^{-/-}$ 293T cells expressing the wild-type IKZF3 degron reporter or a Q147H mutant reporter which is resistant to lenalidomide-induced degradation. Data are normalized to DMSO. **b,** Cell extracts from **a** were applied to $CRBN^{+/+}$ or $CRBN^{-/-}$ cells expressing a full-length IKZF3 reporter. Data are normalized to DMSO. **c,** Treatment with Proteinase K does not diminish CRBN-dependent degradation of the IKZF3 degron reporter induced by cell extracts. Data are normalized to DMSO. **d**, Schema of isolation of eLen activity via co-immunoprecipitation of CRBN and IKZF3 from Molt-4 cells. **e,** FLAG-CRBN was immunoprecipitated with anti-FLAG beads from Molt-4 cells treated with DMSO or glutarimide as depicted in **d**. FLAG-CRBN was eluted with FLAG peptide, crashed in 80% methanol, and a 2 kD filter was used to remove residual protein. Dried down extracts were applied to $CRBN^{+/+}$ or $CRBN^{-/-}$ 293T reporter cells expressing the wild-type IKZF3 degron. Also shown is the bead-only control. **f**, Schema of isolation of eLen activity using whole cell extracts

applied to a recombinant column of CRBN-DDB1 protein produced in insect cells. Tris buffered saline, TBS. **g**, IKZF3-degrading activity present in first TBS washes and two methanol elutions when Molt-4 cell extract was applied to the CRBN column. *** $p<0.001$

Figure 4: eLen induces the recruitment of IKZF1 and CK1α to CRBN and the ubiqutination of IKZF1. a, Design of FRET assay. CRBN mutant is P352G W386A. **b**, Results of TR-FRET assay with IKZF1 using eLen purified from Molt-4 cells. Error bars are standard deviation of ten measurements of the same sample. **c**, TR-FRET assay with CK1α. **d**, Fluorescent IKZF1 ubiquitination assay with eLen. Negative control is lacking E2 enzyme.

Figure 5: Optimization of eLen extraction and creation of solid phase extraction purification methods. a, A number of different metabolite extraction methods from Dietmair et al. (37) and were attempted on two different Molt-4 samples. Standard refers to initial method from Sellick et al (36). The resulting metabolites were dried down and applied to $CRBN^{+/+}$ 293T reporter cells expressing the IKZF3 degron. Data are reported as the ratio of GFP/mCherry normalized to the DMSO condition. **b**, Stability of eLen when subjected to freezing at -80°C or heating to 95°C. Data are normalized to DMSO. **c,** Effect of different extraction volume on eLen yield, reported in lenalidomide-equivalent picomoles. **d,** Lenalidomide-equivalent picomoles of activity present in flow, wash, and elution following SPE purification on an HLB Prime column. **e**, GFP/mCherry ratio in IKZF3 reporter cells treated with eLen eluted from an HLB Prime column using varying percentage of organic solvent (90% acetonitrile (ACN), 10% methanol (MeOH)).

Figure 6: Development of HPLC purification methods for eLen. a, eLen purified from Molt-4 cells by co-immunoprecipitation of CRBN (IP) or three different whole cell extracts (WCE)

have identical retention times. Data are given as the ratio of GFP/mCherry with the DMSO condition normalized to 1. **b-c,** Retention of eLen on an Atlantis T3 column is significantly dependent on the initial solvent conditions. The starting conditions in **b** were 20% acetonitrile, while the starting conditions in **c** were 5% acetonitrile. **d,** Fractionation of eLen with an ammonium formate-based protocol generates two different peaks of eLen activity. These early and late fractions were collected and fractionated again using the same method. **e**, CRBN-dependent IKZF3-degrading activity in eLen produced by a contract research organization (CRO). *** $p<0.0001$. ns, not significant.

Figure 7: Metabolite extracts from Molt-4 cells reduce the post-translational stability of other zinc fingers and have distinct biochemical properties. a, Metabolite extracts from Molt-4 cells were applied to $CRBN^{+/+}$ or $CRBN^{-/-}$ 293T cells expressing the ZNF692 or RNF166 flow-cytometry based reporter. A pomalidomide dose curve is shown for comparison. **b**, Molt-4 cell extracts were subjected to solid phase extraction using an HLB Prime column. The resulting fractions were applied to the indicated reporter cell lines and the relative activity in each fraction was calculated by comparison to a pomalidomide dose curve. Data are shown as the percent of total picomoles of pomalidomide-equivalent activity in each fraction. **c-e** HPLC fractionation of Molt-4 cell extracts demonstrates IKZF3 and RNF166-degrading activity in distinct fractions. Data are shown for several different HPLC methods.

Figure 8: PRISM screen to identify additional cell lines. a, Design of PRISM screen **b,** Results of PRISM screen, expressed as GFP/mCherry ratio of glutarimide 100 μM vs. glutarimide 10 μM treated cells, both normalized to DMSO. Cell pools shown in red were retested. **c,** Results of retest of three of the cell lines. Blue points are results for wild-type IKZF3

degron reporter. Black squares are results for IKZF3-Q147H degron reporter. **d,** Peds005TSusp cells were infected with post-translational stability reporters for the IKZF3 degron or ZFP91 zinc finger 4 and treated with DMSO, glutarimide, or lenalidomide for 18 hours. * $p<0.05$ Histogram from IKZF3 reporter data is shown in **e**. Blue histogram is DMSO treated and red is glutarimide 100 μM. **f**, Effect of 5 hour proteasome inhibitor treatment on post-translational stability of IKZF3 degron and ZFP91 reporters in Peds005TSusp cells. **g**, Peds005TSusp cells expressing Cas9 and the IKZF3 degron reporter were infected at approximately 0.5 multiplicity of infection with BFP^+ vectors containing either a validated CRBN gRNA or a non-targeting guide. After allowing for CRISPR-Cas9 editing, cells were treated with glutarimide or lenalidomide. The GFP/mCherry ratio was compared between the BFP^+ CRISPR-infected cells and the BFP^- CRISPR uninfected cells in each well. **h**, Peds005TSusp cell extracts induce degradation of the IZKF3 degron reporter in $CRBN^{+/+}$ but not $CRBN^{-/-}$ 293T reporter cells. **i**, Peds005TSusp cells expressing a doxycline-inducible SMARCB1 construct and the IKZF3 degron reporter were treated with doxycycline (2 μg/mL) or vehicle and DMSO or glutarimide and the ratio of GFP/mCherry was measured by flow cytometry.

Figure S1: Effect of lenalidomide treatment on $CRBN^{+/+}$ or $CRBN^{-/-}$ 293T cells infected with the 60 amino acid IKZF3 degron reporter.

Figure S2: Names and disease entity of cell lines in re-tested PRISM cell line pools. SCLC, small cell lung cancer. ALL, acute lymphoid leukemia. AML, acute myeloid leukemia.

Figure 1

a

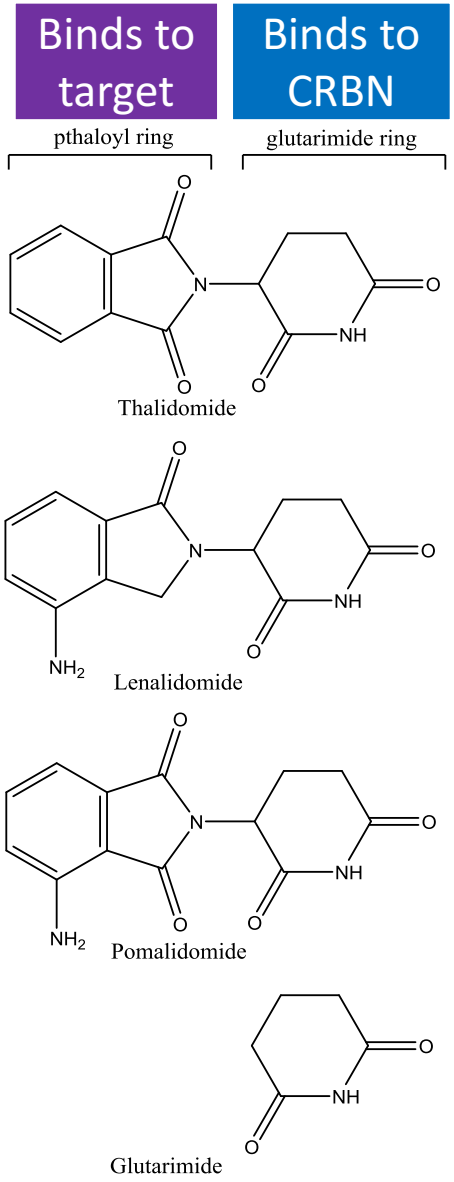

b

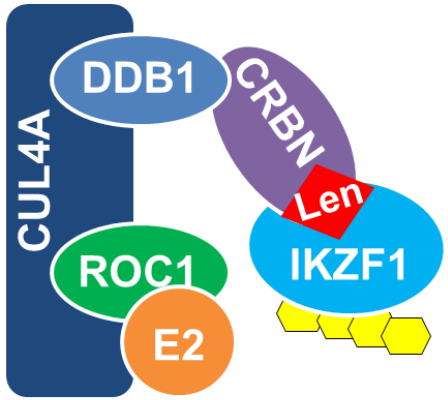

$CRL4^{CRBN}$

Figure 2

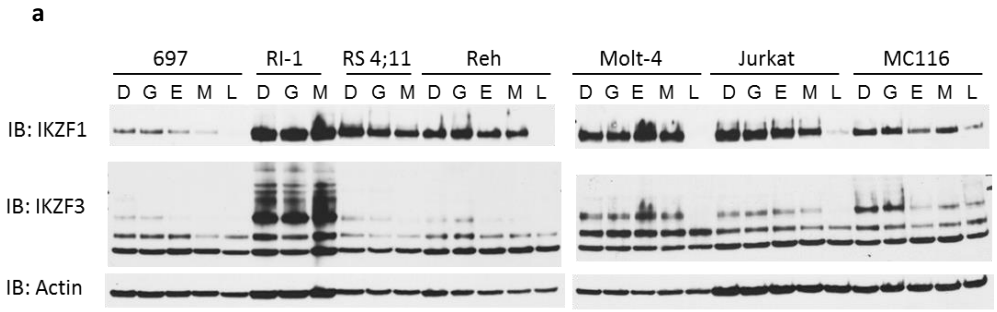
a
697
RI-1
RS 4;11
Reh
Molt-4
Jurkat
MC116
D G E M L D G M D G M D G E M L D G E M L D G E M L D G E M L
IB: IKZF1
IB: IKZF3
IB: Actin


c
SFFV
IKZF3
GFP
IRES
Cherry


e
Molt-4
D G
IB: IKZF1
IB: IKZF3
IB: Actin

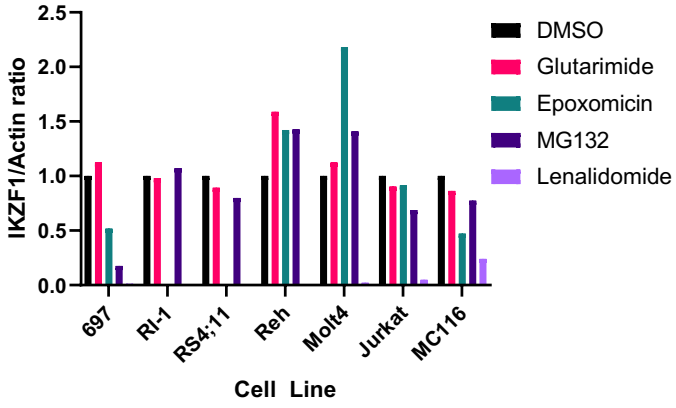
b
IKZF1/Actin ratio
2.5
2.0
1.5
1.0
0.5
0.0
697
RI-1
RS4;11
Reh
Molt4
Jurkat
MC116
Cell Line
DMSO
Glutarimide
Epoxomicin
MG132
Lenalidomide

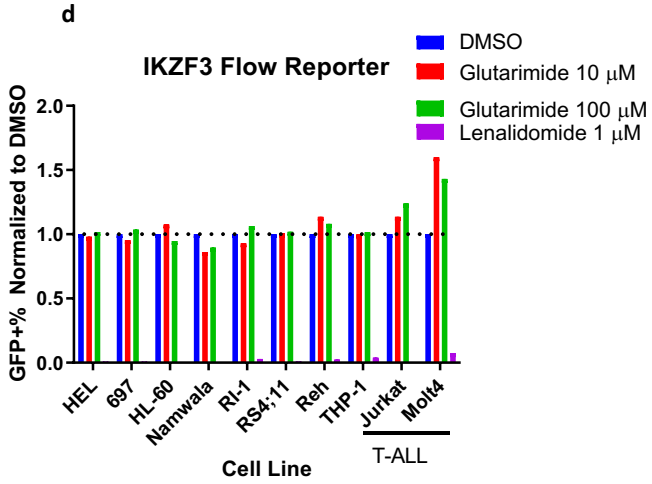
d
IKZF3 Flow Reporter
GFP+% Normalized to DMSO
2.0
1.5
1.0
0.5
0.0
HEL
697
HL-60
Namwala
RI-1
RS4;11
Reh
THP-1
Jurkat
Molt4
T-ALL
Cell Line
DMSO
Glutarimide 10 μM
Glutarimide 100 μM
Lenalidomide 1 μM

Figure 3

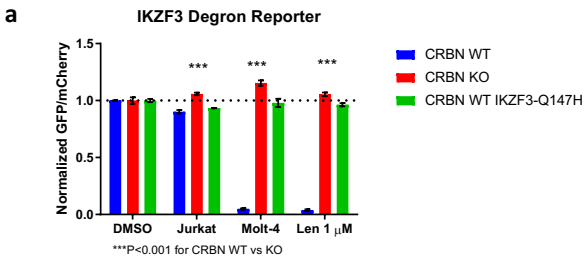
a
IKZF3 Degron Reporter
Normalized GFP/mCherry
1.5
1.0
0.5
0.0
***
***
***
DMSO
Jurkat
Molt-4
Len 1 μM
***P<0.001 for CRBN WT vs KO
CRBN WT
CRBN KO
CRBN WT IKZF3-Q147H

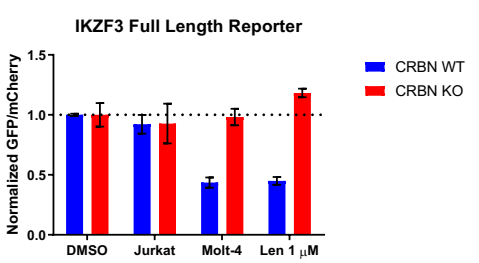
b
IKZF3 Full Length Reporter
Normalized GFP/mCherry
1.5
1.0
0.5
0.0
DMSO
Jurkat
Molt-4
Len 1 μM
CRBN WT
CRBN KO

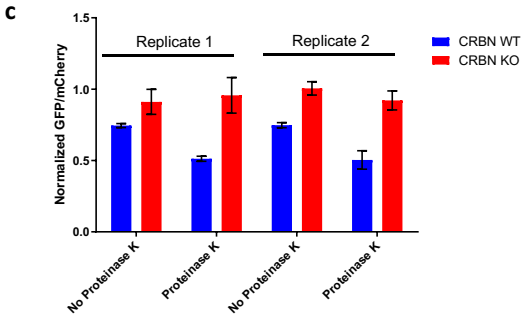
c
Replicate 1
Replicate 2
Normalized GFP/mCherry
1.5
1.0
0.5
0.0
No Proteinase K
Proteinase K
No Proteinase K
Proteinase K
CRBN WT
CRBN KO

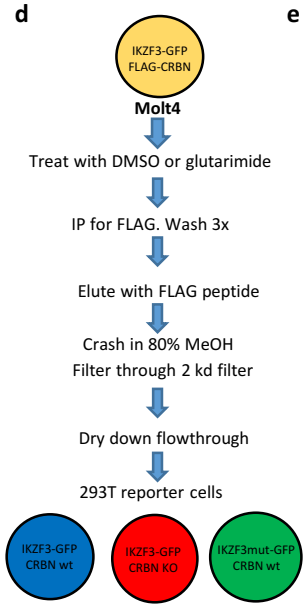
d
IKZF3-GFP
FLAG-CRBN
Molt4
Treat with DMSO or glutarimide
IP for FLAG. Wash 3x
Elute with FLAG peptide
Crash in 80% MeOH
Filter through 2 kd filter
Dry down flowthrough
293T reporter cells
IKZF3-GFP
CRBN wt
IKZF3-GFP
CRBN KO
IKZF3mut-GFP
CRBN wt

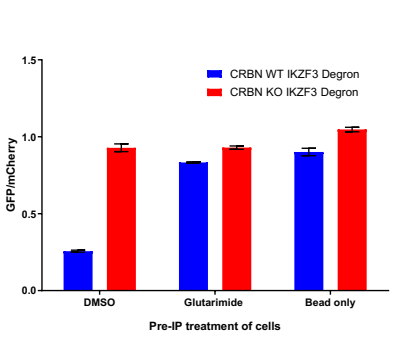
e
GFP/mCherry
1.5
1.0
0.5
0.0
DMSO
Glutarimide
Bead only
Pre-IP treatment of cells
CRBN WT IKZF3 Degron
CRBN KO IKZF3 Degron

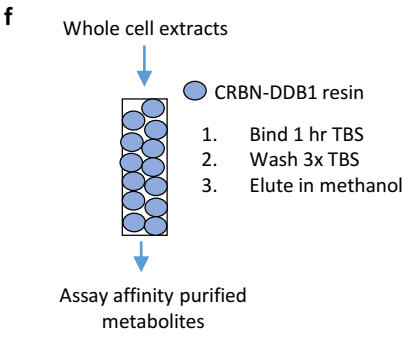
f
Whole cell extracts
CRBN-DDB1 resin
1. Bind 1 hr TBS
2. Wash 3x TBS
3. Elute in methanol
Assay affinity purified
metabolites

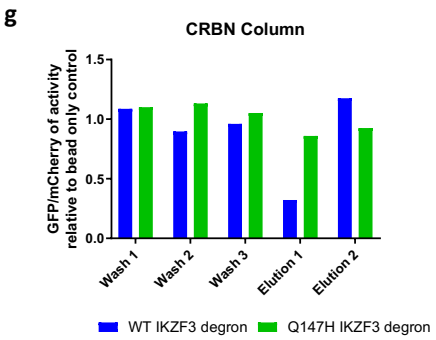
g
CRBN Column
GFP/mCherry of activity
relative to bead only control
1.5
1.0
0.5
0.0
Wash 1
Wash 2
Wash 3
Elution 1
Elution 2
WT IKZF3 degron
Q147H IKZF3 degron

Figure 4

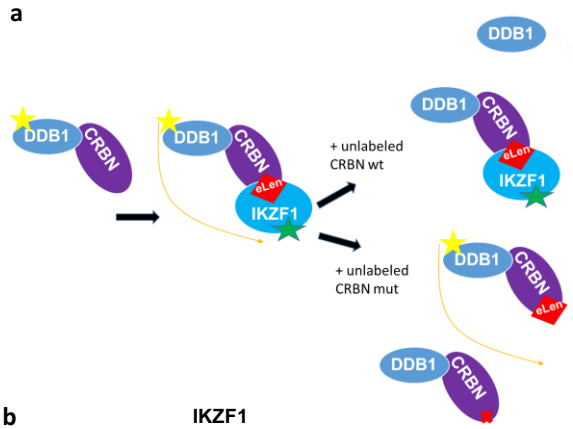

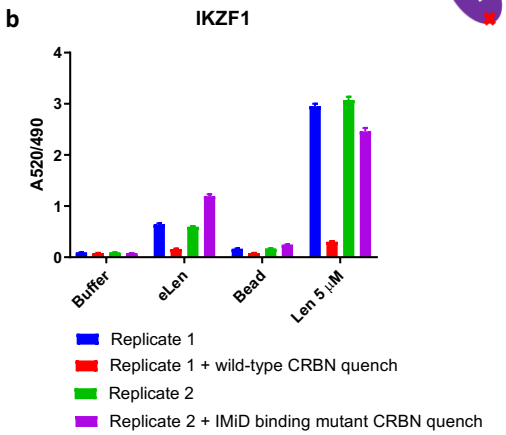

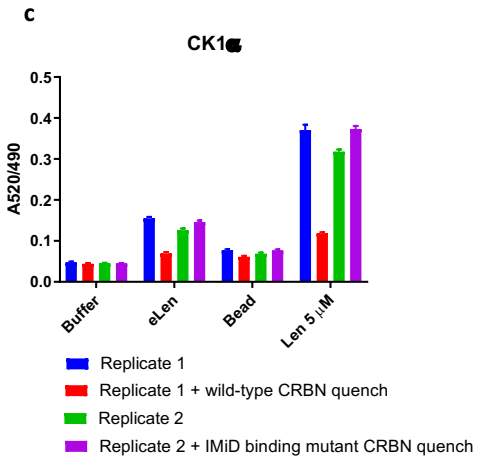

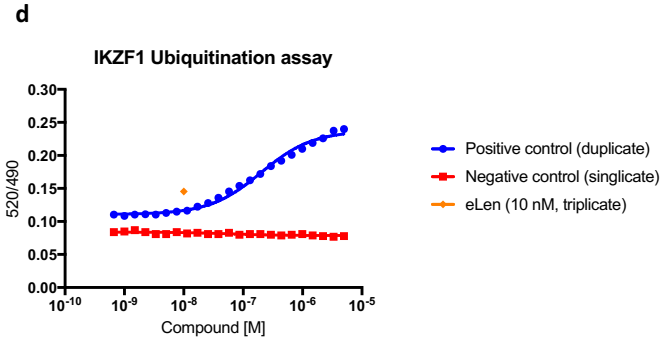

	Positive control (duplicate)
EC50	2.013e-007

Figure 5

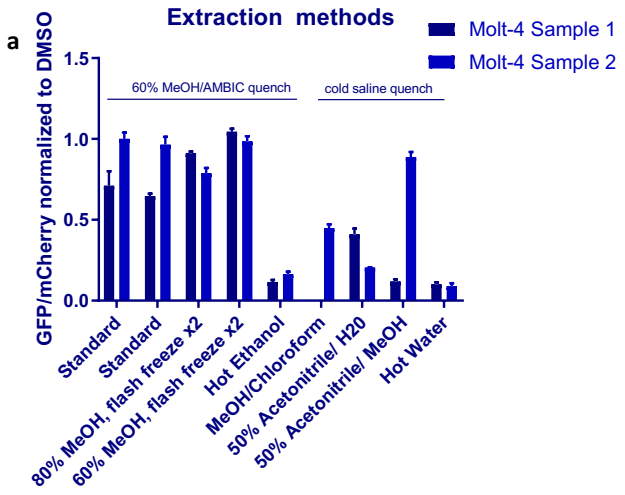
a
Extraction methods
Molt-4 Sample 1
Molt-4 Sample 2
GFP/mCherry normalized to DMSO
60% MeOH/AMBIC quench
cold saline quench
Standard
Standard
80% MeOH, flash freeze x2
60% MeOH, flash freeze x2
Hot Ethanol
MeOH/Chloroform
50% Acetonitrile/ H20
50% Acetonitrile/ MeOH
Hot Water

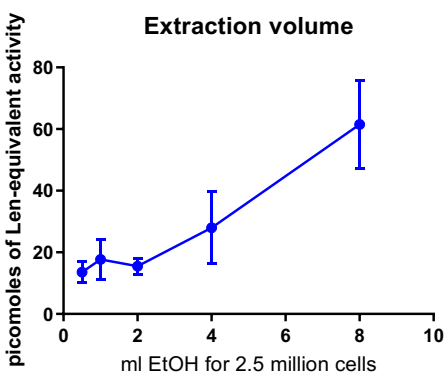
c
Extraction volume
picomoles of Len-equivalent activity
ml EtOH for 2.5 million cells

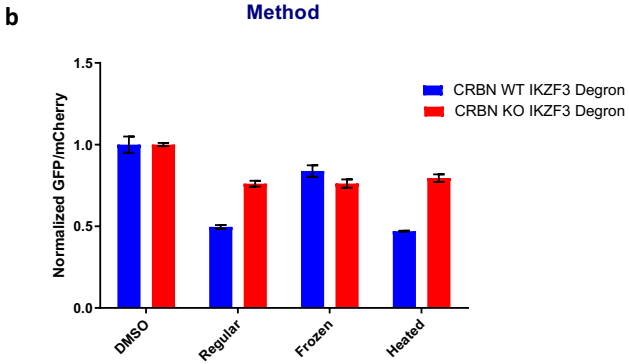
b
Method
CRBN WT IKZF3 Degron
CRBN KO IKZF3 Degron
Normalized GFP/mCherry
DMSO
Regular
Frozen
Heated

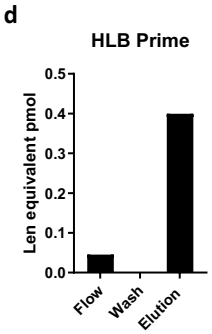
d
HLB Prime
Len equivalent pmol
Flow
Wash
Elution

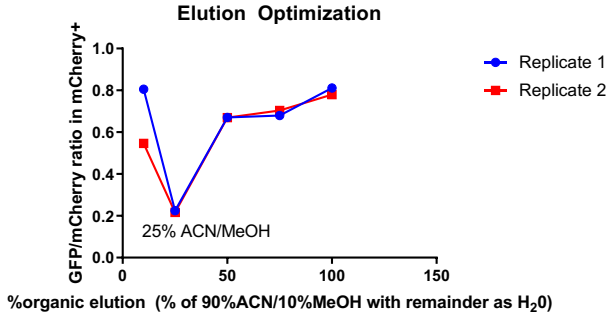
e
Elution Optimization
Replicate 1
Replicate 2
GFP/mCherry ratio in mCherry+
25% ACN/MeOH
%organic elution (% of 90%ACN/10%MeOH with remainder as H20)

Figure 6

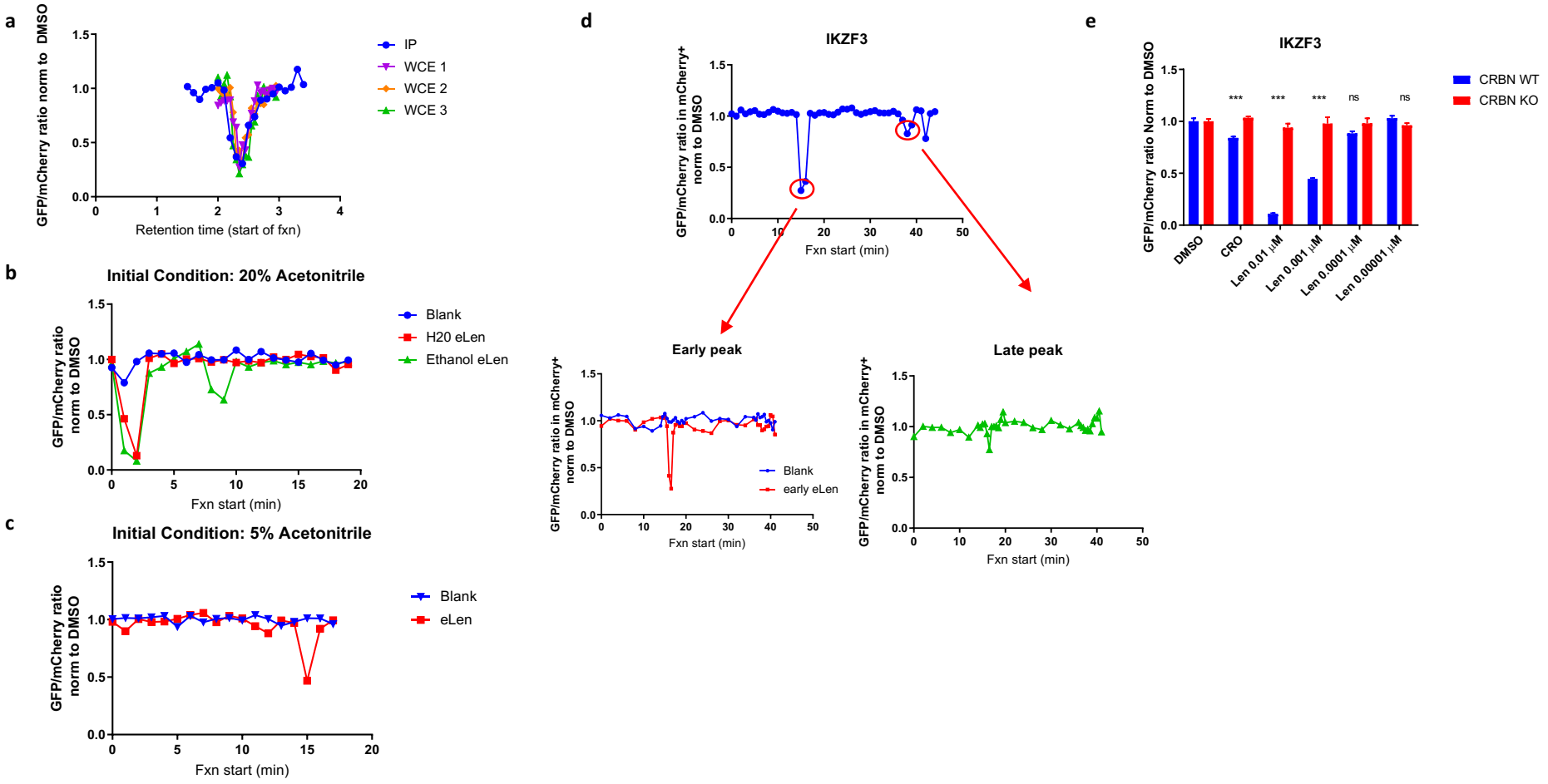
a
GFP/mCherry ratio norm to DMSO
Retention time (start of fxn)
IP
WCE 1
WCE 2
WCE 3
b
Initial Condition: 20% Acetonitrile
GFP/mCherry ratio norm to DMSO
Fxn start (min)
Blank
H20 eLen
Ethanol eLen
c
Initial Condition: 5% Acetonitrile
GFP/mCherry ratio norm to DMSO
Fxn start (min)
Blank
eLen
d
IKZF3
GFP/mCherry ratio in mCherry+ norm to DMSO
Fxn start (min)
Early peak
Late peak
Blank
early eLen
e
IKZF3
GFP/mCherry ratio Norm to DMSO
CRBN WT
CRBN KO
***
***
***
ns
ns
DMSO
CRO
Len 0.01 μM
Len 0.001 μM
Len 0.0001 μM
Len 0.00001 μM

Figure 7

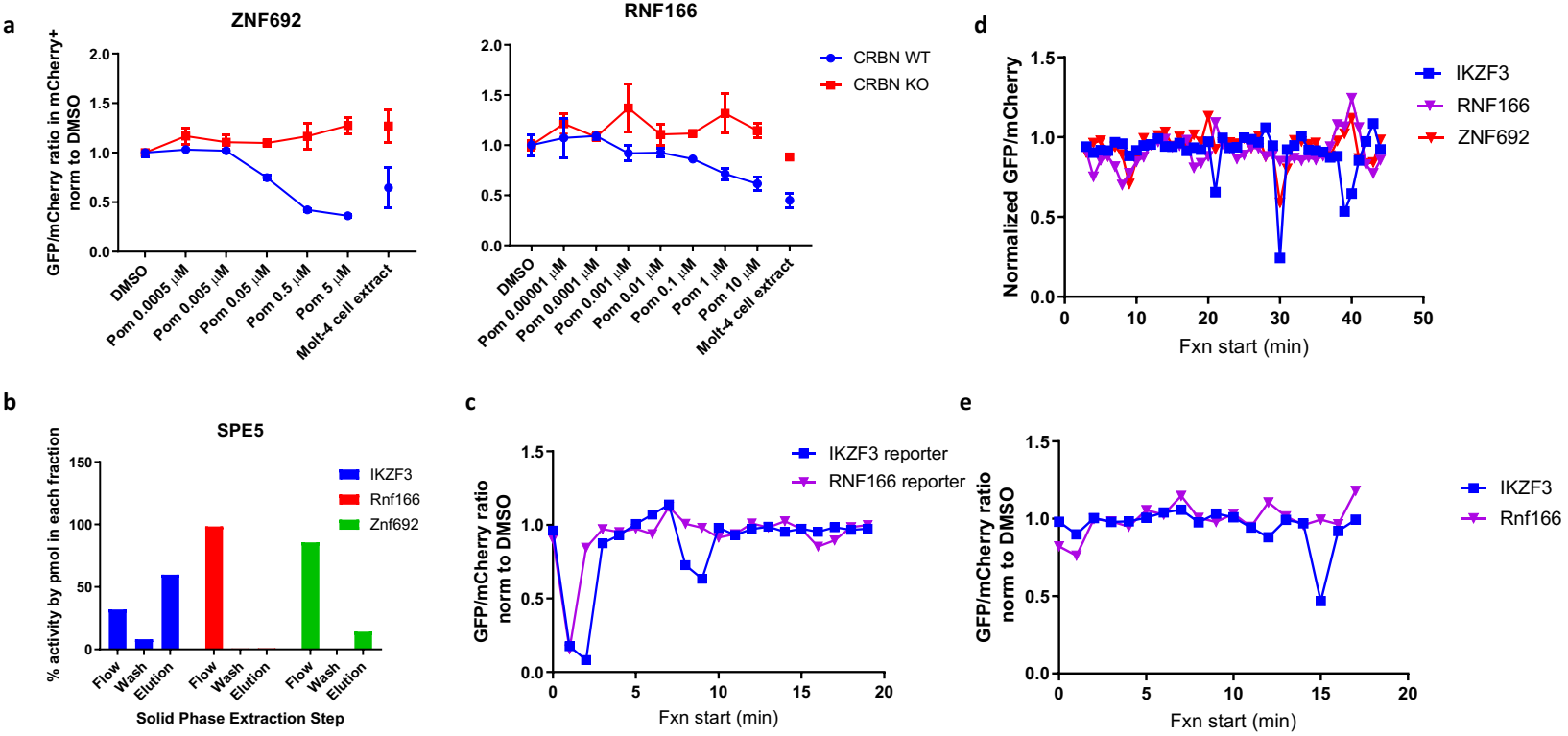
a
ZNF692
GFP/mCherry ratio in mCherry+ norm to DMSO
DMSO
Pom 0.0005 μM
Pom 0.005 μM
Pom 0.05 μM
Pom 0.5 μM
Pom 5 μM
Molt-4 cell extract
RNF166
CRBN WT
CRBN KO
Pom 0.00001 μM
Pom 0.0001 μM
Pom 0.001 μM
Pom 0.01 μM
Pom 0.1 μM
Pom 1 μM
Pom 10 μM
d
Normalized GFP/mCherry
IKZF3
RNF166
ZNF692
Fxn start (min)
b
SPE5
% activity by pmol in each fraction
IKZF3
Rnf166
Znf692
Flow
Wash
Elution
Solid Phase Extraction Step
c
GFP/mCherry ratio norm to DMSO
IKZF3 reporter
RNF166 reporter
Fxn start (min)
e
GFP/mCherry ratio norm to DMSO
IKZF3
Rnf166
Fxn start (min)

Figure 8

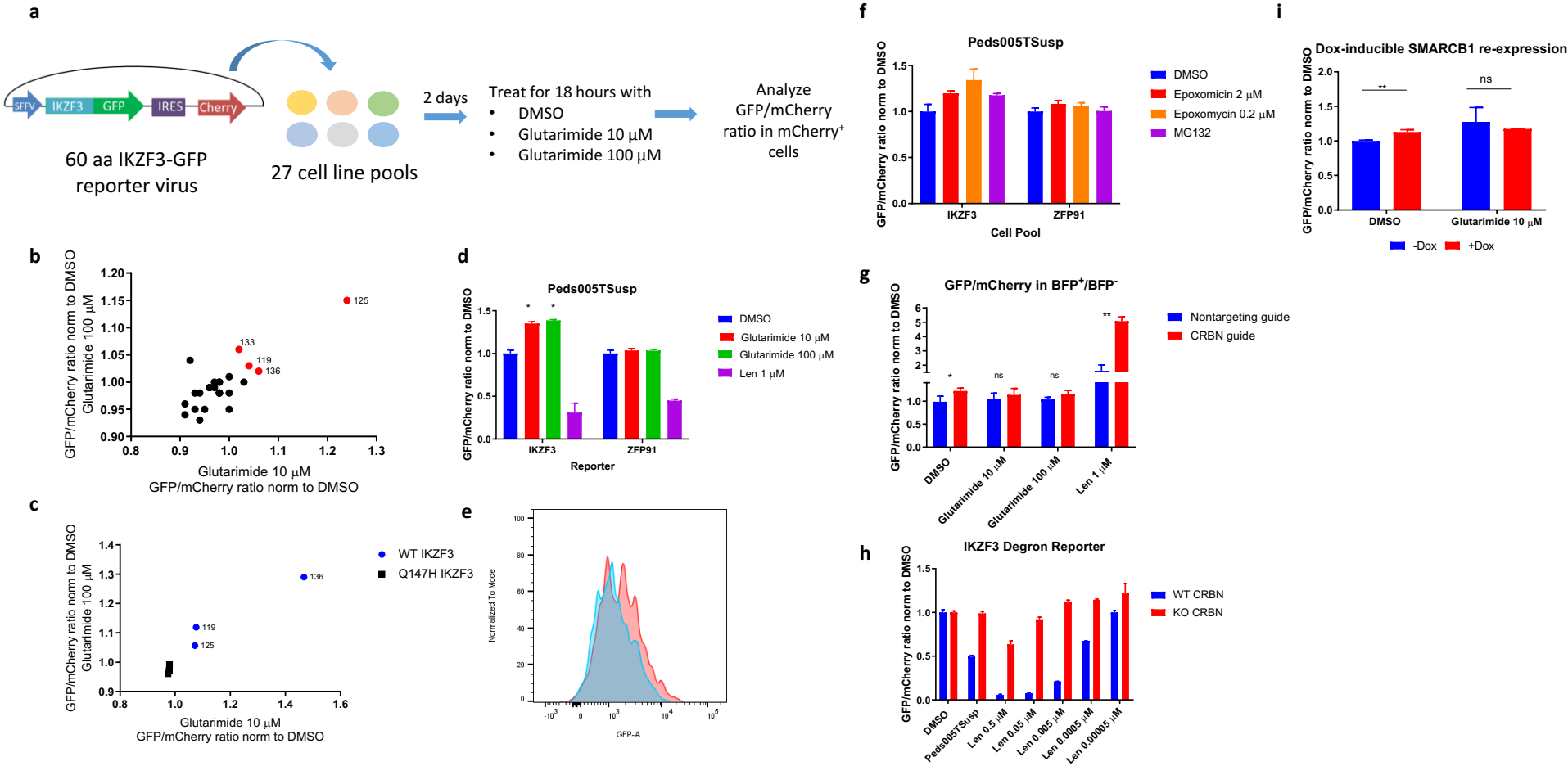
a
SFFV
IKZF3
GFP
IRES
Cherry
60 aa IKZF3-GFP reporter virus
27 cell line pools
2 days
Treat for 18 hours with
DMSO
Glutarimide 10 µM
Glutarimide 100 µM
Analyze GFP/mCherry ratio in mCherry+ cells
b
GFP/mCherry ratio norm to DMSO Glutarimide 100 µM
Glutarimide 10 µM GFP/mCherry ratio norm to DMSO
125
133
119
136
c
GFP/mCherry ratio norm to DMSO Glutarimide 100 µM
Glutarimide 10 µM GFP/mCherry ratio norm to DMSO
WT IKZF3
Q147H IKZF3
119
125
136
d
Peds005TSusp
GFP/mCherry ratio norm to DMSO
IKZF3
ZFP91
Reporter
DMSO
Glutarimide 10 µM
Glutarimide 100 µM
Len 1 µM
e
Normalized To Mode
GFP-A
f
Peds005TSusp
GFP/mCherry ratio norm to DMSO
IKZF3
ZFP91
Cell Pool
DMSO
Epoxomicin 2 µM
Epoxomycin 0.2 µM
MG132
g
GFP/mCherry in BFP+/BFP-
GFP/mCherry ratio norm to DMSO
DMSO
Glutarimide 10 µM
Glutarimide 100 µM
Len 1 µM
Nontargeting guide
CRBN guide
h
IKZF3 Degron Reporter
GFP/mCherry ratio norm to DMSO
DMSO
Peds005TSusp
Len 0.5 µM
Len 0.05 µM
Len 0.005 µM
Len 0.0005 µM
Len 0.00005 µM
WT CRBN
KO CRBN
i
Dox-inducible SMARCB1 re-expression
GFP/mCherry ratio norm to DMSO
DMSO
Glutarimide 10 µM
-Dox
+Dox

Figure S1

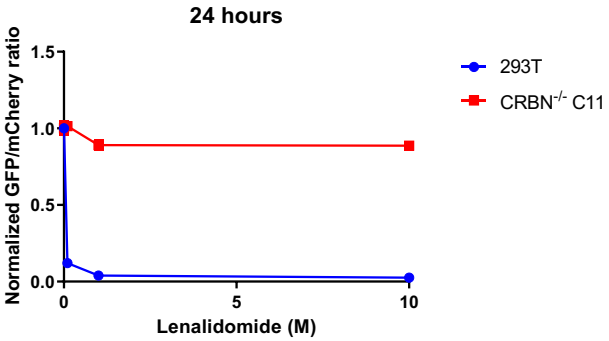
24 hours
Normalized GFP/mCherry ratio
1.5
1.0
0.5
0.0
0
5
10
Lenalidomide (M)
293T
CRBN-/- C11

Figure S2

Pool 125	
Peds005T Susp	Kidney Cancer
COR-L88	SCLC
NCI-H1092	SCLC
NCI-H1341	SCLC
NCI-H2171	SCLC

Pool 119	
GDM-1	AML
OCI-AML5	AML
PL-21	AML
SKM-1	AML
THP-1	AML

Pool 133	
ALL-SIL	ALL
C8166	ALL
JM1	ALL
EOL-1	AML
KHM-1B	Multiple Myeloma

Pool 136	
CAL-148	Breast Cancer
ECC10	Gastric Cancer
KATO III	Gastric Cancer
BT-12	Rhabdoid Cancer